

Deployment and Trajectory Optimization of UAVs: A Quantization Theory Approach

Maryam Shabanighazikelayeh, Erdem Koyuncu, and Hulya Seferoglu
Department of Electrical and Computer Engineering, University of Illinois at Chicago

Abstract—Optimal deployment and movement of multiple unmanned aerial vehicles (UAVs) is studied. The scenarios of variable data rate with fixed transmission power, and variable transmission power with fixed data rate are considered. First, the optimal deployment of UAVs is studied for the static case of a fixed ground terminal (GT) density. Using high resolution quantization theory, the corresponding best achievable performance (average data rate or transmission power) is determined in the asymptotic regime of a large number of UAVs. Next, the dynamic case where the GT density is allowed to vary periodically through time is considered. For one-dimensional networks, an accurate formula for the total amount of UAV movement that guarantees the best time-averaged performance is determined. In general, the tradeoff between the total UAV movement and the achievable performance is obtained through a Lagrangian approach. A corresponding trajectory optimization algorithm is introduced and shown to guarantee a convergent Lagrangian. Numerical simulations are also carried out to confirm the analytical findings.

I. INTRODUCTION

Unmanned aerial vehicles (UAVs) can be effectively utilized in a variety of wireless communication scenarios. Example applications include providing coverage to geographical areas lacking a wireless infrastructure, relaying to overcome terrain obstacles such as mountains, improving cell edge performance by creating femtocells, among many others [1], [2].

One of the most distinguishing features of UAV networks is the opportunity of very fast dynamic adaptation to the ever-changing environment through relocation. Environmental variations in this context may include ground terminal (GT) location/density variations, UAV node failures, etc. Although the ability of relocation potentially offers significant performance gains, including improved coverage and rate for GTs, it also comes with many theoretical and practical challenges. Even in a static scenario where the locations or the density of GTs are known and fixed, finding the optimal UAV locations is a non-convex optimization problem whose dimensionality grows with the number of UAVs [1]. Dynamic scenarios further involve optimization of UAV trajectories, thus leading to much more complicated infinite-dimensional optimization problems.

Several approaches to resolve the challenges of UAV deployment/relocation have been proposed. In the case of static deployment, [3]–[5] consider the optimal placement of UAVs to maximize coverage and propose several algorithms. These works assume that a UAV can cover a GT provided that they are separated no more than a certain distance.

There are also numerous studies on dynamic deployment of UAVs. Algorithms for UAV coverage under variable coverage radii and possible UAV losses are proposed in [6]. For a single UAV and one GT, [7] studies trajectory optimization in order to achieve high throughput with low UAV energy

consumption. For a single source-destination pair and one UAV, [8] develops a mobile UAV relaying method. The goal is throughput maximization via jointly optimizing UAV trajectory and temporal power allocation. In both [7] and [8], the free-space path-loss model has been considered. A genetic algorithm for UAV trajectory optimization has been proposed in [9] with the specific goal of restoring network service after natural disasters. The utilization of UAVs as relays between GTs and a central base station has been studied in [10], and a joint heading and adaptive handoff algorithm is proposed. In [11], the authors consider trajectory optimization for a single UAV serving multiple mobile GTs using space-division multiple access. A Kalman filter predicts the future GT locations, which, in turn, determine the UAV trajectory.

Despite many recent studies on UAV deployment and trajectory optimization, some of which have been described above, there are many fundamental questions that are yet to be answered. In particular, for static networks, there is no general analytical framework that can provide the optimal UAV positions for a given number of UAVs and spatial user density. Also, for the dynamic scenario, most of the above work relies on numerical methods for optimizing UAV trajectories and determining the resulting performance.

Quantization theory of data compression and source coding [12] has proved to be a very successful analytical tool in addressing many existing problems that involve geographical deployment of agents [13]; examples applications of the theory include the deployment of antenna arrays [14], sensors [15], or general heterogeneous nodes [16]. The main contribution of this paper is to show that many of the aforementioned open problems on UAV networks can as well be formulated and ultimately resolved using quantization theory. In particular, we determine the optimal static UAV deployments for any given density function of the GTs. For one-dimensional dynamic networks, we obtain the first closed-form expressions for the optimal UAV trajectories and the resulting performance gains.

The rest of this paper is organized as follows: In Section II, we introduce the system model. We analyze the static and dynamic deployment scenarios in Sections III and IV, respectively. We provide numerical simulation results in Section V. Finally, in Section VI, we draw our main conclusions and discuss extensions to variable-rate transmission. Part of this work will be presented in a conference [17].

II. SYSTEM MODEL

We consider a network of several GTs at zero elevation and several UAVs at a fixed elevation $h > 0$. Mathematically, we assume that the GTs are located on \mathbb{R}^d , where $d \in \{1, 2\}$.

While typically one is interested in the case $d = 2$, i.e. when the GTs are in general positions on the ground, the case $d = 1$ is also relevant: The GTs may be constrained to lie on a line on the ground, e.g. as cars on a straight highway.

We distinguish between what we refer to as the static and the dynamic deployment scenarios. In static deployment, we assume that the GTs are located on \mathbb{R}^d according to a certain fixed (time-invariant) density function f , where $\int_{\mathbb{R}^d} f(q) dq = 1$. In the more complicated dynamic deployment scenario, we will allow the user density to vary over time.

A. Static Deployment

In order to formally describe the static deployment scenario, let $x_1, \dots, x_n \in \mathbb{R}^d$ denote the UAVs' (projected) locations on the GT space. The squared Euclidean distance between a GT at q and the i th UAV at x_i is then given by $\|x_i - q\|^2 + h^2$. Fig. 1 provides an illustration for the special case of $n = d = 2$.

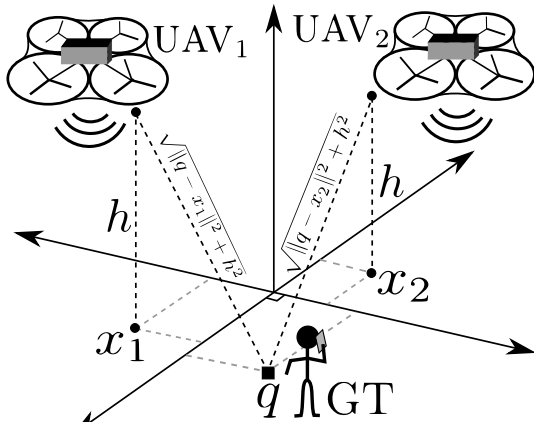


Fig. 1. A network of two UAVs serving a GT.

We first consider fixed-rate variable-power transmission at GTs. The case of fixed-power variable-rate transmission will be discussed later. Suppose that a GT at location q wishes to communicate with rate ρ bits/sec/Hz, and transmits with power P . Due to the aerial nature of the communication system, we assume that there is line of sight between the GTs and the UAVs, and the effects of multipath fading is negligible. In such a scenario, the received signal power at a UAV at x_i is given by $(\|x_i - q\|^2 + h^2)^{-\frac{\alpha}{2}} P$, where α is the path loss exponent. Reliable communication between the GT and the UAV is possible provided that the capacity of the (Gaussian) channel between the GT and the UAV is at least ρ , or, mathematically $\log_2(1 + (\|x_i - q\|^2 + h^2)^{-\frac{\alpha}{2}} P) \geq \rho$. The minimum transmission power of a GT at q that guarantees reliable data reception at a UAV at x_i is then $\frac{\rho}{P} (\|x_i - q\|^2 + h^2)^{\frac{\alpha}{2}}$. The minimum transmission power that guarantees successful data reception at at least one of the UAVs is therefore $\min_i \frac{\rho}{P} (\|x_i - q\|^2 + h^2)^{\frac{\alpha}{2}}$. Averaging out the user density, and setting $\rho = P = 1$ without loss of generality, the average transmission power of GTs given UAV locations $\mathbf{x} \triangleq [x_1 \dots x_n]$ and GT density f is

$$P(\mathbf{x}, f) \triangleq \int_{\mathbb{R}^d} \min_i (\|x_i - q\|^2 + h^2)^{\frac{\alpha}{2}} f(q) dq. \quad (1)$$

The static deployment problem is then to find the optimal UAV locations that minimize the average GT power consumption. In other words, we wish to determine $P^*(f) \triangleq \min_{\mathbf{x}} P(\mathbf{x}, f)$, and the optimal deployments \mathbf{x}^* that achieve $P(\mathbf{x}^*, f) = P^*(f)$.

B. Dynamic Deployment

In practice, the GT density may vary with time. For example, in daily urban communications, the GT density over highways will be higher during rush hours, when compared to nighttime. In order to model such scenarios, we let f_t denote the GT density function at time t . We assume f_t is periodic over a time interval of length T , i.e. $f_t(q) = f_{t+T}(q)$, $\forall t, \forall q$. For example, one may set $T = 24$ hours for the urban communication scenario. We also assume that $f_t(q)$ is continuous in both t and q . In other words, the GT density does not experience abrupt changes over space or time.

Let $x_{i,t}$ denote the location of UAV i at time t , and $\mathbf{x}_t = [x_{t,1} \dots x_{t,n}]$ denote the vector of UAV locations at time t . The power consumption of GTs at time t is $P(\mathbf{x}_t, f_t)$. The average power consumption over time can be expressed as

$$Q \triangleq \frac{1}{T} \int_0^T P(\mathbf{x}_t, f_t) dt. \quad (2)$$

We have omitted to indicate the dependency of Q on $\{(\mathbf{x}_t, f_t) : t \in [0, T]\}$ for brevity. The time-averaged distance traversed by the i th UAV can be calculated to be the line integral

$$M_i \triangleq \frac{1}{T} \int_0^T \sqrt{\sum_{j=1}^d \left| \frac{\partial x_{t,i,j}}{\partial t} \right|^2} dt, \quad (3)$$

where $x_{t,i,j}$ represents the j th component of $x_{t,i}$. The goal is to find the optimal UAV trajectories that minimize the average GT power consumption Q subject to a constraint $\sum_{i=1}^n M_i \leq M$ on the total UAV movement, where $M \geq 0$ is given.

III. OPTIMIZATION OF A STATIC DEPLOYMENT

We begin with the simpler scenario of a static deployment and its optimization. Namely, we study the minimization of (1) with respect to UAV locations \mathbf{x} . We begin by considering the degenerate case $h = 0$, in which case we can imagine that the network consists of unmanned ground vehicles (UGVs) instead of UAVs. The analysis of such a UGV scenario will be very useful for our analysis of the UAV case $h > 0$.

A. The UGV Case $h = 0$

For $h = 0$, the cost function in (1) becomes

$$P(\mathbf{x}, f) = \int_{\mathbb{R}^d} \min_i \|x_i - q\|^r f(q) dq, \quad h = 0. \quad (4)$$

This expression is the well-known average r th power distortion of a quantizer whose reproduction points are x_1, \dots, x_n for a given source density f . Finding the exact minimizers of (4) and the corresponding minimum distortions is possible only for a few special cases. In particular, if $f(q) = \mathbf{1}(q \in [0, 1])$ is the one-dimensional uniform density, then the optimal reproduction points are given by the uniform quantizer codebook $\mathbf{x}_u = [\frac{1}{2n} \frac{3}{2n} \dots \frac{2n-1}{2n}]$ with $P(\mathbf{x}_u, f) = \frac{1}{(1+r)(2n)^r}$.

For a general uniform density, we have the following result. Given $A \subset \mathbb{R}^d$, let $m(A) \triangleq \int_A \|q\|^r dq / (\int_A dq)^{\frac{d+r}{d}}$ denote the normalized moment of A .

Proposition 1 (Zador [18]). *Let $f(q) = \mathbf{1}(q \in [0, 1]^d)$, $h = 0$. As $n \rightarrow \infty$, we have $P^*(f) = \kappa_{rd} n^{-\frac{r}{d}} + o(n^{-\frac{r}{d}})$, where κ_{rd} depends only on r and d . In particular, $\kappa_{r1} = \frac{2^{-r}}{1+r}$ and κ_{r2} are the normalized moments of the origin-centered interval and the origin-centered regular hexagon, respectively.*

This implies in particular that for two dimensions and a uniform distribution, the best arrangement of quantization points is asymptotically the regular hexagonal lattice.

Making the transition from uniform to non-uniform f can be accomplished using the idea of point density functions. In detail, one assumes the existence of a function $\lambda(q)$ such that the cube $[q, q + dq]$ of volume dq contains $n\lambda(q)dq$ reproduction points with $\int_{\mathbb{R}^d} \lambda(q)dq = 1$. Since f should be approximately uniform on $[q, q + dq]$, the conditional average distortion on $[q, q + dq]$ is $\kappa_{rd}(n\lambda(q))^{-\frac{r}{d}}$ by Proposition 1. Averaging out the density, we obtain the formula

$$\tilde{P}(\lambda) \triangleq \kappa_{rd} n^{-\frac{r}{d}} \int_{\mathbb{R}^d} f(q) \lambda^{-\frac{r}{d}}(q) dq + o(n^{-\frac{r}{d}}). \quad (5)$$

for the average distortion given the point density function λ . Using reverse Hölder's inequality, we have

$$\tilde{P}(\lambda) \geq \kappa_{rd} n^{-\frac{r}{d}} \|f\|_{\frac{d}{d+r}} + o(n^{-\frac{r}{d}}), \quad (6)$$

where $\|f\|_\alpha \triangleq (\int_{\mathbb{R}^d} (f(q))^\alpha dq)^{\frac{1}{\alpha}}$. In (6), equality holds if

$$\lambda(q) = f^{\frac{d}{d+r}}(q) / \int_{\mathbb{R}^d} f^{\frac{d}{d+r}}(q') dq'. \quad (7)$$

Therefore, the minimum distortion $\kappa_{rd} n^{-\frac{r}{d}} \|f\|_{\frac{d}{d+r}} + o(n^{-\frac{r}{d}})$ is achieved by the point density function in (7).

B. The UAV Case $h > 0$

We now consider the case $h > 0$. We begin with the simple case of a uniform one-dimensional distribution.

Proposition 2. *Let $f(q) = \mathbf{1}(q \in [0, 1])$. A minimizer of (1) is the uniform quantizer codebook \mathbf{x}_u . The corresponding minimum average power is $P(\mathbf{x}_u, f) = 2n \int_0^{\frac{1}{2n}} (u^2 + h^2)^{\frac{r}{2}} du$.*

Proof. First, note that if g is monotonically increasing, $A \subset \mathbb{R}$, and $x \in \mathbb{R}$, we have $\int_A g(\|x - q\|) dq \geq \int_B g(\|q\|) dq$, where B is the origin-centered interval with the same measure as A . In particular, for $g(u) = (u^2 + h^2)^{\frac{r}{2}}$, we obtain

$$\int_A (\|x - q\|^2 + h^2)^{\frac{r}{2}} dq \geq h(\mu(A)), \quad (8)$$

where $h(\nu) \triangleq \int_{-\frac{1}{2}\nu}^{\frac{1}{2}\nu} (u^2 + h^2)^{\frac{r}{2}} du = 2 \int_0^{\frac{1}{2}\nu} (u^2 + h^2)^{\frac{r}{2}} du$, and $\mu(A)$ is the Lebesgue measure of A . By differentiation, it can be shown that $h(\nu)$ is a concave function of ν . Now, let $V_i \triangleq \{q : \|q - x_i\| \leq \|q - x_j\|, \forall j\}$, $i = 1, \dots, n$ denote the Voronoi cells that are generated by x_1, \dots, x_n . We have

$$P(\mathbf{x}, f) = \sum_{i=1}^n \int_{V_i} (\|x_i - q\|^2 + h^2)^{\frac{r}{2}} dq \quad (9)$$

$$\geq \sum_{i=1}^n h(\mu(V_i)) \geq nh \left(\frac{1}{n} \sum_{i=1}^n \mu(V_i) \right) \quad (10)$$

$$= nh \left(\frac{1}{n} \right) = 2n \int_0^{\frac{1}{2n}} (u^2 + h^2)^{\frac{r}{2}} du. \quad (11)$$

The first and the second inequalities follow from (8) and the concavity of $h(\cdot)$, respectively. It can easily be verified that the last expression equals $P(\mathbf{x}_u, f)$. This concludes the proof. \square

For a general d and f , we observe that if x_1, \dots, x_n is an optimal deployment, then the set of points q with the property that $\min_i \|q - x_i\| \rightarrow 0$ as $n \rightarrow \infty$ should have probability 1 (The formal proof is technical and is thus omitted for brevity.). This amounts to the intuitive observation that every GT should be allocated a closer UAV as the number of available UAVs grows to infinity. As a result, we may use the Taylor series expansion $(\min_i \|x_i - q\|^2 + h^2)^{\frac{r}{2}} = h^r + \frac{1}{2} r h^{r-2} \min_i \|x_i - q\|^2 + o(\min_i \|x_i - q\|^2)$ so that, substituting to (1), we have

$$P(\mathbf{x}, f) = h^r + \frac{1}{2} r h^{r-2} \int_{\mathbb{R}^d} \min_i \|x_i - q\|^2 f(q) dq + \int_{\mathbb{R}^d} o(\min_i \|x_i - q\|^2) f(q) dq. \quad (12)$$

Using (6) and (7), we can then obtain the following theorem.

Theorem 1. *As $n \rightarrow \infty$, we have*

$$P^*(f) = \begin{cases} \kappa_{rd} n^{-\frac{r}{d}} \|f\|_{\frac{d}{d+r}} + o(n^{-\frac{r}{d}}), & h=0, \\ h^r + \frac{r h^{r-2} \kappa_{2d}}{2} n^{-\frac{r}{d}} \|f\|_{\frac{d}{d+2}} + o(n^{-\frac{r}{d}}), & h>0. \end{cases} \quad (13)$$

The optimal point density function is given by

$$\lambda^*(q; f) \triangleq \begin{cases} f^{\frac{d}{d+r}}(q) / \int_{\mathbb{R}^d} f^{\frac{d}{d+r}}(q') dq', & h=0, \\ f^{\frac{d}{d+2}}(q) / \int_{\mathbb{R}^d} f^{\frac{d}{d+2}}(q') dq', & h>0. \end{cases} \quad (14)$$

This provides a complete asymptotic characterization of the achievable GT power consumption and the corresponding optimal UAV configuration.

IV. OPTIMIZATION OF A DYNAMIC DEPLOYMENT

We now consider the dynamic scenario, where the GT density varies periodically over time. As discussed in Section II-B, the goal in this case is to minimize the time-averaged power consumption Q in (2), subject to the constraint $\sum_{i=1}^n M_i \leq M$ on the total movement of UAVs. Here, M_i denotes the total movement of the i th UAV, and has been defined in (3). Given $M \geq 0$, we use the notation $Q^*(M)$ to denote the minimum of (2) subject to $\sum_{i=1}^n M_i \leq M$. We first consider the two extremal cases $M = 0$ and $M \rightarrow \infty$.

A. No UAV movement: $M = 0$

The case $M = 0$ corresponds to a scenario where we do not allow any UAV movement. Equivalently, the UAV locations are fixed over time as $\mathbf{x}_t = \mathbf{x}'$, $\forall t$ for a collection $\mathbf{x}' = [x'_1 \dots x'_n]$ of UAV locations to be optimized. By (1) and (2), we have

$$Q^*(0) = \min_{\mathbf{x}'} \frac{1}{T} \int_0^T \int_{\mathbb{R}^d} \min_i (\|x'_i - q\|^2 + h^2)^{\frac{r}{2}} f_t(q) dq dt. \quad (15)$$

Now, let $\bar{f}(q) \triangleq \frac{1}{T} \int_0^T f_t(q) dt$ be the ‘‘time-averaged density.’’ Note that $\int_{\mathbb{R}^d} \bar{f}(q) dq = 1$ so that \bar{f} is a valid density function. According to (1) and (15), we have $Q^*(0) = \min_{\mathbf{x}'} P(\mathbf{x}', \bar{f})$, and optimizing over \mathbf{x}' leads to the following.

Proposition 3. *We have $Q^*(0) = P^*(\bar{f})$.*

Note that Theorem 1 can be applied to provide an asymptotically tight expression for $P^*(\bar{f})$ (and thus $Q^*(0)$).

Example 1. Let us consider a one-dimensional network $d = 1$, a period of length $T = 2$ with path loss exponent $r = 2$. For a simpler exposition, we further consider an UGV network where $h = 0$. Let the time-varying GT density be given by

$$f_t(q) = (1+3|t|)(q-2+2|t|)^{3|t|},$$

$$q \in [2-2|t|, 3-2|t|], t \in [-1, 1]. \quad (16)$$

This defines time-shifted power-law densities. For example for $t = -1$, we obtain the density $f_1(q) = 4q^3$, $q \in [0, 1]$, and for $t = 0$, we obtain $f_0(q) = 1$, $q \in [2, 3]$. The time-averaged density \bar{f} as well as its $\frac{1}{3}$ -norm $\|\bar{f}\|_{\frac{1}{3}} \approx 6.08$ can be found by numerical integration. By Proposition 3 and Theorem 1, it follows that $Q^*(0) \approx \frac{6.08}{12} n^{-2} = 0.507n^{-2}$. The optimal point (UAV) density function is given by $\lambda_2^*(\bar{f})$. \square

B. Unlimited UAV movement: $M \rightarrow \infty$

We now allow an unlimited amount of UAV movement so as to obtain the minimum possible time-averaged GT power consumption. For this purpose, at each time t , we use the UAV locations that provide the minimum “instantaneous” GT power consumption. This results in the time-averaged power

$$Q^*(\infty) = \frac{1}{T} \int_0^T P^*(f_t) dt. \quad (17)$$

We recall that Theorem 1 provides an asymptotic expression for the integrand $P^*(f_t)$. This can be substituted to (17) for an asymptotically tight characterization of $Q^*(\infty)$.

We now argue that (17) is, in fact, achievable with a finite amount of total movement as well. In other words, there is a constant $\bar{M} > 0$ such that $Q^*(M) = Q^*(\infty)$ for every $M \geq \bar{M}$. The idea is to observe that the GT density f_t at time t is not “vastly different” than the GT density f_{t+dt} at time $t + dt$. This stems from our practical assumption in Section II-B that the spatiotemporal density $f_t(q)$ is continuous in both space and time. As a result, we expect the optimal location for each UAV to be a well-behaved continuous function of time, resulting in a finite amount of total UAV movement.

We utilize high-resolution quantization theory to estimate \bar{M} . The key is to recover the location of each UAV at any given point t in time through the optimal quantizer point density function at time t . Namely, let $\mathbf{x}_t^* \triangleq [x_{t,1}^* \cdots x_{t,n}^*]$ denote the optimal UAV locations at time t for density f_t . We first consider the case of one dimension $d = 1$. Without loss of generality, suppose $x_{t,1}^* \leq \cdots \leq x_{t,n}^*$. Given $x \in [0, 1]$, let $\Lambda_{\text{inv}}^*(x; f_t)$ be the unique real number that satisfies

$$\int_0^{\Lambda_{\text{inv}}^*(x; f_t)} \lambda^*(q; f_t) dq = x, \quad (18)$$

where $\lambda^*(q; f_t)$ is the optimal point density function for f_t , as defined in Theorem 1. Note that $\Lambda_{\text{inv}}^*(x; f_t)$ is the inverse of

the cumulative distribution function $u \rightarrow \int_0^u \lambda^*(q; f_t) dq$. Our idea is to approximate the optimal UAV locations via

$$x_{t,i}^* \simeq \tilde{x}_{t,i} \triangleq \Lambda_{\text{inv}}^* \left(\frac{2i-1}{2n}; f_t \right), i = 1, \dots, n. \quad (19)$$

Note that if U is a random variable that is uniformly distributed on $[0, 1]$, then, according to the inverse transform sampling method, the random variable $\Lambda_{\text{inv}}^*(U; f_t)$ is distributed according to the density function $\lambda^*(q; f_t)$. The transformation in (19) can thus be considered to be a “deterministic version” of inverse transform sampling, where the uniform random variable U is replaced with the uniform quantizer with reproduction points $\frac{2i-1}{2n}$, $i = 1, \dots, n$. The resulting estimates $\tilde{x}_{t,i}$ is consistent with the density function $\lambda^*(q; f_t)$ in the sense that for every q and $\epsilon > 0$, the fraction of $\tilde{x}_{t,i}$ that is on $(q, q + \epsilon)$ converges to $\lambda^*(q; f_t)\epsilon$ as $n \rightarrow \infty$.

Substituting (19) to (3), we obtain the following result.

Theorem 2. Let $d = 1$. As $n \rightarrow \infty$, the minimum possible average power consumption of $Q^*(\infty) = \frac{1}{T} \int_0^T P^*(f_t)$ is achievable with a total movement of

$$\bar{M}_i \triangleq \frac{1}{T} \int_0^T \left| \frac{\partial \Lambda_{\text{inv}}^*(x; f_t)}{\partial t} \right| dt \quad (20)$$

for the i th UAV. Correspondingly, $\bar{M} = \sum_{i=1}^n \bar{M}_i$.

Example 2. We continue the setup in Example 1. By Theorems 1 and 2, we can calculate $Q^*(\infty) = \frac{1}{16n^2} + o\left(\frac{1}{n^2}\right)$. In order to estimate \bar{M} , we calculate $\lambda^*(q, f_t) = (1+|t|)(q-2+2|t|)^{|t|}$ so that $\tilde{x}_{t,i} = 2-2|t| + \left(\frac{2i-1}{2n}\right)^{\frac{1}{1+|t|}}$ and $\bar{M}_i = 2 + \left(\frac{2i-1}{2n}\right)^{\frac{1}{2}} - \frac{2i-1}{2n}$. Thus, the power consumption of $Q^*(\infty)$ is achievable with a total UAV movement of $\bar{M} = 2n + \sum_{i=1}^n \left(\frac{2i-1}{2n} - \left(\frac{2i-1}{2n}\right)^{\frac{1}{2}}\right)$. The optimal UAV trajectories are given by $\tilde{x}_{t,i}$.

The arguments above are not immediately applicable to the case of two dimensions. The main difficulty is to find a simple analogue of (19) that can faithfully extract the optimal UAV locations from the optimal UAV density functions. We leave a resolution of this problem as future work. Nevertheless, \bar{M} and $Q^*(\bar{M})$ can still be numerically approximated for two dimensional densities as we show in Section V.

C. Moderate UAV movement: $0 < M < \bar{M}$

We now consider the achievable performance between the two extremal cases of no UAV movement and unlimited UAV movement. We combine the power consumption (objective) function Q in (2) and the movement (constraint) function $\sum_{i=1}^n M_i$ through the Lagrangian

$$Q + \ell \sum_{i=1}^n M_i = \frac{1}{T} \int_0^T \left[P(\mathbf{x}_t, f_t) + \ell \sum_{i=1}^n \sqrt{\sum_{j=1}^d \left| \frac{\partial x_{t,i,j}}{\partial t} \right|^2} \right] dt. \quad (21)$$

Minimizing the Lagrangian for different values of the Lagrange multiplier $\ell > 0$ enables travel over the $(M, Q^*(M))$ tradeoff curve: For example, a small ℓ does not penalize the total amount of movement as much as a larger ℓ does. It thus results in a lower power consumption compared to the case of

a larger ℓ , albeit at the expense of more movement. The formulation in (21) is thus similar to the Lagrangian formulation of the entropy-constrained quantizer design problem [19].

Minimizing the Lagrangian in (21) requires optimization over the uncountably infinitely many variables $x_{t,i}$, $t \in [0, T]$, $i \in \{1, \dots, n\}$, and is thus infeasible. The first step towards a feasible optimization is to discretize the continuous time interval $[0, T]$ to the set of discrete time instances $\{0, \frac{T}{K}, \frac{2T}{K}, \dots, \frac{(K-1)T}{K}\}$, where $K \geq 2$ is a natural number. This results in the discrete-time Lagrangian

$$\mathcal{L} \triangleq \frac{1}{K} \sum_{k=0}^{K-1} P(\mathbf{y}_k, \hat{f}_k) + \ell \sum_{k=0}^{K-1} \sum_{i=1}^n \|y_{k,i} - y_{((k-1) \bmod K),i}\|, \quad (22)$$

where the discrete time k corresponds to the continuous time $\frac{kT}{K}$, and the optimization is over $\mathbf{y}_k \triangleq \mathbf{x}_{\frac{kT}{K}} = [y_{k,1} \dots y_{k,n}]$ with density $\hat{f}_k \triangleq f_{\frac{kT}{K}}$. It can be shown that if $x_{t,i}$, $i = 1, \dots, n$ are continuous in t , the discrete time Lagrangian converges to the continuous time Lagrangian as the number of time steps K grows to infinity. We thus expect the minimizers of (22) to also coincide asymptotically as $K \rightarrow \infty$. Still, the direct minimization of (22) is a dnK dimensional optimization problem. In order to further reduce the dimensionality, we define

$$\mathcal{L}_k \triangleq \frac{1}{K} P(\mathbf{y}_k, \hat{f}_k) + \ell \sum_{i=1}^n \|y_{k,i} - y_{((k-1) \bmod K),i}\| + \ell \sum_{i=1}^n \|y_{k,i} - y_{((k+1) \bmod K),i}\|, \quad k = 1, \dots, K, \quad (23)$$

and note that $\mathcal{L} - \mathcal{L}_k$ does not depend on \mathbf{y}_k . The gradient of \mathcal{L}_k with respect to $y_{k,i}$ can be calculated as

$$\frac{\partial \mathcal{L}_k}{\partial y_{k,i}} = \frac{r}{K} \int_{\mathcal{V}_{k,i}} (\|y_{k,i} - q\|^2 + h^2)^{\frac{r}{2}-1} (y_{k,i} - q) \hat{f}_k(q) dq + \ell \frac{y_{k,i} - y_{((k-1) \bmod K),i}}{\|y_{k,i} - y_{((k-1) \bmod K),i}\|} + \ell \frac{y_{k,i} - y_{((k+1) \bmod K),i}}{\|y_{k,i} - y_{((k+1) \bmod K),i}\|}, \quad (24)$$

where $\mathcal{V}_{k,i} \triangleq \{q : \|y_{k,i} - q\| \leq \|y_{k,j} - q\|, \forall j \in \{1, \dots, n\}\}$ is the Voronoi cell of the i th UAV at time k . We now consider the following algorithm: We begin with an initial (e.g., random) guess on $\mathbf{y}_0, \dots, \mathbf{y}_{K-1}$. For the infinite sequence of indices $k = 0, 1, \dots, K-1, 0, 1, \dots, K-1, \dots$, we minimize \mathcal{L}_k over \mathbf{y}_k through gradient descent, while keeping all \mathbf{y}_i , $i \neq k$ fixed. Since each step minimizes \mathcal{L}_k over \mathbf{y}_k for some $k \in \{0, \dots, K-1\}$, and the dependence of \mathcal{L} on \mathbf{y}_k is only through \mathcal{L}_k , the process guarantees a decreasing (and thus convergent) \mathcal{L} . In fact, in our numerical experiments, we have observed that the algorithm provides convergent trajectories as well. A formal proof of this observation will remain as an interesting direction for future research.

We also note that one can also consider a minimization of (23) based on Lloyd algorithm [20], [21]. In fact, we have

$$\mathcal{L}_k = \frac{1}{K} \sum_{i=1}^n \int_{\mathcal{V}_{k,i}} (\|y_{k,i} - q\|^2 + h^2)^{\frac{r}{2}} \hat{f}_k(q) dq + \ell \sum_{i=1}^n (\|y_{k,i} - y_{((k-1) \bmod K),i}\| + \|y_{k,i} - y_{((k+1) \bmod K),i}\|), \quad (25)$$

This expression depends on $y_{k,i}$ only through

$$\mathcal{L}_{k,i} \triangleq \frac{1}{K} \int_{\mathcal{V}_{k,i}} (\|y_{k,i} - q\|^2 + h^2)^{\frac{r}{2}} \hat{f}_k(q) dq + \ell \|y_{k,i} - y_{((k-1) \bmod K),i}\| + \ell \|y_{k,i} - y_{((k+1) \bmod K),i}\|. \quad (26)$$

Given that $\mathcal{V}_{k,i}$, $i = 1, \dots, n$ are kept fixed, $\mathcal{L}_{k,i}$ is a convex function of $y_{k,i}$ and thus be effectively minimized using any convex optimization method, or gradient descent. Once each $\mathcal{L}_{k,i}$, $i = 1, \dots, n$ are minimized (while keeping $\mathcal{V}_{k,i}$, $i = 1, \dots, n$ fixed), the new Voronoi regions $\mathcal{V}_{k,i}$, $i = 1, \dots, n$ will be calculated according to the new $y_{k,i}$, $i = 1, \dots, n$. The algorithm proceeds in this iterative manner until convergence. Since each optimization we have described results in a lower \mathcal{L}_k , the algorithm, in fact, converges in a cost function sense.

Minimization of (26) may become potentially even simpler for some special cases. In fact, for $r = 2$, the minimization can easily be shown to be equivalent to minimizing

$$y_{k,i} \mapsto \frac{1}{K} \mu(\mathcal{V}_{k,i}) \|y_{k,i} - \overline{V}_{k,i}\|^2 + \ell \|y_{k,i} - y_{((k-1) \bmod K),i}\| + \ell \|y_{k,i} - y_{((k+1) \bmod K),i}\|, \quad (27)$$

where

$$\overline{V}_{k,i} \triangleq \frac{\int_{\mathcal{V}_{k,i}} q \hat{f}_k(q) dq}{\int_{\mathcal{V}_{k,i}} \hat{f}_k(q) dq} \quad (28)$$

is the geometric centroid of $V_{k,i}$ with respect to density \hat{f}_k . We can thus also avoid integration over the generally complicated region $\mathcal{V}_{k,i}$. We can also greatly reduce the search space for $y_{k,i}$ as shown in the following. For a simpler notation, given $u, v, w, x \in \mathbb{R}^d$ and $c > 0$ let us first define

$$\phi(x) = \|x - u\| + \|x - v\| + c\|x - w\|^2. \quad (29)$$

Note that the minimization of (27) is equivalent to the minimization of (29) for appropriately chosen vectors u, v, w . We need the following lemma.

Lemma 1. *Let $T \subset \mathbb{R}^d$ be a triangle with vertices u, v, w , including its interior. Let $x \in \mathbb{R}^d$ be arbitrary. There exists $y \in T$ such that $y \ll x$, where “ $y \ll x$ ” is the shorthand notation for conditions $\|y - u\| \leq \|x - u\|$, $\|y - v\| \leq \|x - v\|$, and $\|y - w\| \leq \|x - w\|$.*

Proof. If $x \in T$, we set $y = x$, and the proof is complete. Otherwise, let x_0 be the projection of x on the two-dimensional subspace that contains T . We have $x_0 \ll x$ by the Pythagorean inequality. If $x_0 \in T$, the lemma then follows with $y = x_0$. Otherwise, by appropriate translations of vectors u, v, w, x_0 ,

we may assume that $u = \begin{bmatrix} 0 \\ 0 \end{bmatrix}$, $v = \begin{bmatrix} v_1 \\ 0 \end{bmatrix}$, $w = \begin{bmatrix} w_1 \\ w_2 \end{bmatrix}$, and $x_0 = \begin{bmatrix} x_{01} \\ x_{02} \end{bmatrix}$, where $v_1, x_{01}, x_{02} \geq 0$, $w_2 \leq 0$, and $w_1 \in \mathbb{R}$. Now, let $x_1 = \begin{bmatrix} x_{01} \\ 0 \end{bmatrix}$. The geometry so far is illustrated in Fig. 2. It is easily verified that $\|x_1 - u\| \leq \|x_0 - u\|$ and

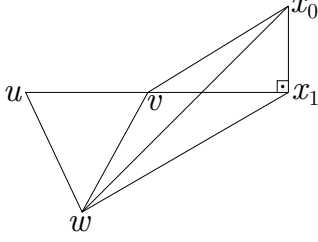


Fig. 2. The first case for the proof of Lemma 1.

$\|x_1 - v\| \leq \|x_0 - v\|$. Also, since the angle $\widehat{x_0x_1w}$ is at least 90° , we have $\|x_1 - w\| \leq \|x_0 - w\|$, and therefore, $x_1 \ll x_0$. If $x_1 \in T$, the lemma then holds for $y = x_1$. Otherwise, we consider the following three cases: The first case $w_1 \leq v_1$ is the same scenario as illustrated in Fig. 2. In this case, we have $v \ll x_1$, and since $v \in T$ obviously, the proof is complete with $y = v$. The second case $v_1 \leq w_1 \leq x_{01}$ is illustrated in Fig. 3. We let $x_2 = \begin{bmatrix} w_1 \\ 0 \end{bmatrix}$, and x_3 to be the projection of x_2 on the edge vw . The relation $x_2 \ll x_1$ obviously holds. The relation

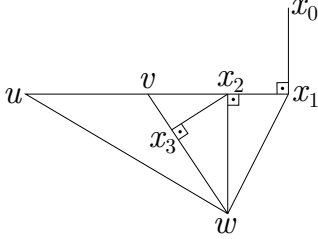


Fig. 3. The second case for the proof of Lemma 1.

$x_3 \ll x_2$ follows from the same arguments that we have used to prove $x_1 \ll x_0$ in Fig. 2. Since $x_3 \in T$, the lemma follows with $y = x_3$. Finally, for the third case $w_1 \geq x_{01}$, let x_4 to be the projection of x_1 on the edge vw . The proof of the relation $x_4 \ll x_1$ similarly follows the proof of $x_1 \ll x_0$ in Fig. 2. The lemma then holds for $y = x_4$. This concludes the proof. \square

We now have the following proposition.

Proposition 4. *A minimizer of x^* of (29) lies on the triangle T with vertices u, v, w .*

Proof. Suppose $x^* \notin T$. By Lemma 1, we can find $y \in T$ such that $\|y - a\| \leq \|x^* - a\|$ for every vertex a of T . It follows that y is also a minimizer of (29). \square

Therefore, without loss of optimality, we may minimize (29) over all x of the form $x = w + \alpha x' + \beta x''$, where $\alpha, \beta \geq 0$, $\alpha + \beta \leq 1$, and $x' = u - w$, $x'' = v - w$ are triangle edge vectors. Hence, the minimization of (29), which should take place over the entire \mathbb{R}^d , can be transformed to a convex optimization over the (two-dimensional) triangle $\alpha, \beta \geq 0$, $\alpha + \beta \leq 1$.

In the special case of one dimension, (29) can also be solved exactly, as shown by the following proposition.

Proposition 5. *Let $d = 1$, and $x^* = \arg \min_{x \in \mathbb{R}^d} \phi(x)$. For a simpler notation, we define the intermediate variables*

$$u' \triangleq \min\{u, v\}, \quad (30)$$

$$v' \triangleq \max\{u, v\}, \quad (31)$$

$$\alpha \triangleq \min \left\{ \left| w - \frac{u+v}{2} \right|, \frac{1}{c} \right\}. \quad (32)$$

We have

$$x^* = \begin{cases} w, & w \in [u', v'], \\ \max\{v', w - \alpha\}, & w > v', \\ \min\{u', w + \alpha\}, & w < u'. \end{cases} \quad (33)$$

Proof. Let $\phi_1(x) = |x - u| + |x - v|$ and $\phi_2(x) = c|x - w|^2$. Without loss of generality, let $u \leq v$. We have $\phi_1(x) \geq v - u$ with equality if and only if $x \in [u, v]$, and $\phi_2(x) \geq 0$ with equality if and only if $x = w$. Therefore, $\phi(x) \geq v - u$ with equality if and only if $x = w$ and $x \in [u, v]$, or equivalently, if $x = w$ and $w \in [u, v]$. This proves the first case in (33).

Suppose $w > v$. We first show that $x^* \in [v, w]$. We have $x^* \in [u, w]$ by Lemma 1. Moreover, for any $x \in [u, v]$, we have $\phi(x) = v - u + c|x - w|^2 \geq v - u + c|v - w|^2$ with equality if and only if $x = v$. Hence, $x^* \in [u, v]$ implies $x^* = v$. Combining with $x^* \in [u, w]$ yields $x^* \in [v, w]$.

Now, let $\xi(x) = |2x - u - v| + c|x - w|^2$. We have $\xi(x) \leq \phi(x)$ for all $x \in \mathbb{R}$. Equality holds if and only if $x \leq u$ or $x \geq v$. Let $y^* = \arg \min_{x \in \mathbb{R}} \xi(x)$ denote the global minimizer of ξ . According to [22], we have

$$y^* = (w - \alpha) \in [u, w]. \quad (34)$$

If further $y^* \in [v, w]$, we have

$$y^* = \arg \min_{x \in [v, w]} \xi(x) = \arg \min_{x \in [v, w]} \phi(x) \quad (35)$$

$$= \arg \min_{x \in \mathbb{R}} \phi(x) = x^*. \quad (36)$$

Otherwise, if $y^* \leq v$, first note that ξ is increasing on $[v, \infty)$ as ξ is convex. It follows that ϕ is increasing on $[v, \infty)$. Since $x^* \in [v, w]$ as already shown, ϕ attains its minimum at $x^* = v$. Hence, we have $x^* = \max\{v, y^*\} = \max\{v', w - \alpha\}$ in general, and this proves the second case in (33). The final case in (33) follows from the same arguments. \square

V. NUMERICAL RESULTS

In this section, we provide numerical simulations that use gradient descent and verify our analytical results. We first proceed with the setup in Examples 1 and 2 for the special case of $n = 10$ UAVs. Let us first consider the case of unlimited UAV movement for minimum average power consumption. In Fig. 4, we compare the analytical optimal trajectories (as derived in Example 2) to that of numerically optimal trajectories as found using gradient descent for the UAVs. Also, we have normalized both the analytical and the simulation trajectories by subtracting the time-varying drift $2 - 2|t|$ of the density function. We can observe that, for

any UAV index, the analysis matches the simulation very well. For the same setup, in Fig. 5, the curve with label ‘‘Simulation’’ illustrates the tradeoff between the total UAV movement and average GT power consumption. In order to obtain the curve, we have used the algorithm in Section IV-C with different values of the Lagrange multiplier ℓ . A time discretization of $K = 200$ is used. The two points labeled as ‘‘Analysis’’ are the analytical approximations to the extremal points $(0, Q^*(0))$ and $(\bar{M}, Q^*(\infty))$ as determined in Examples 1 and 2, respectively. We can observe that both points match almost perfectly with the simulation results.

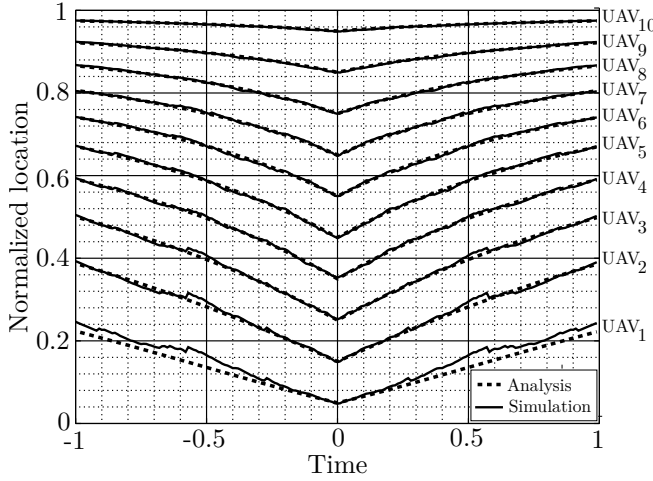


Fig. 4. Trajectories of 10 UAVs in a one-dimensional network.

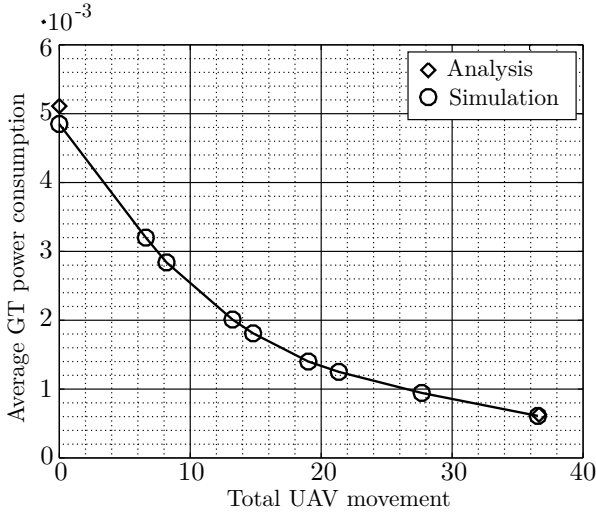


Fig. 5. Total movement vs. power consumption for a one-dimensional network.

As an example of two-dimensional ($d=2$) dynamic deployment, let f_t be the density function of the random variable $(3+2\sin 2\pi t)N+2[\sin 2\pi t \ \cos 2\pi t]$, where N is a Gaussian random vector with identity covariance matrix. Hence, f_t is Gaussian at any t and its mean and variance varies periodically over time with $T = 1$. We consider $n = 4$ UAVs, a path loss exponent of $r = 3$, UAV height $h = 1$, and $K = 100$

discrete time instances. In Fig. 6, we show the optimized UAV trajectories for two different Lagrange multipliers $\ell \in \{0, 0.1\}$. The corresponding total movements and power consumptions are shown in Fig. 7 along with the data of 5 other trajectories that are obtained using different Lagrange multipliers. As expected, a larger ℓ provides a shorter trajectory but larger average GT power consumption. Also, the obtained data points in Fig. 7 suggest that the tradeoff curve is convex. The lower number of UAVs in this scenario means that the asymptotic results in Theorems 1 and 2 will not be as accurate as when applied to the one-dimensional scenario considered earlier. For example, by Fig. 7, the simulated value for the minimum average power consumption is $Q^*(\bar{M}) \simeq 42$ with $\bar{M} \simeq 61$, while Theorem 2 provides the estimate $Q^*(\bar{M}) \simeq 17$. Such mismatch is often observed in other results based on high-resolution quantization theory (see, e.g., [16], [18]), and will disappear for a large number of UAVs.

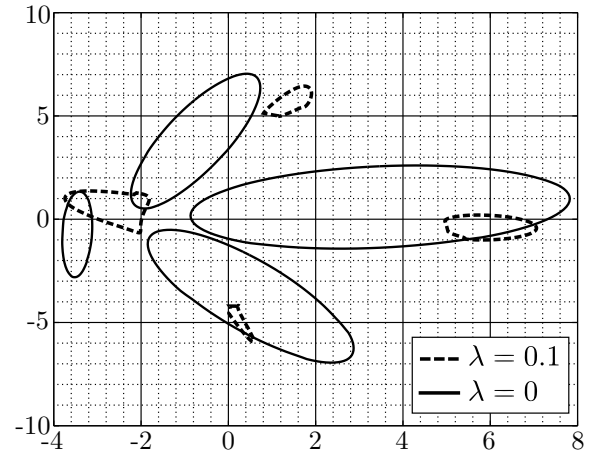


Fig. 6. Two different trajectories of 4 UAVs in a two-dimensional network.

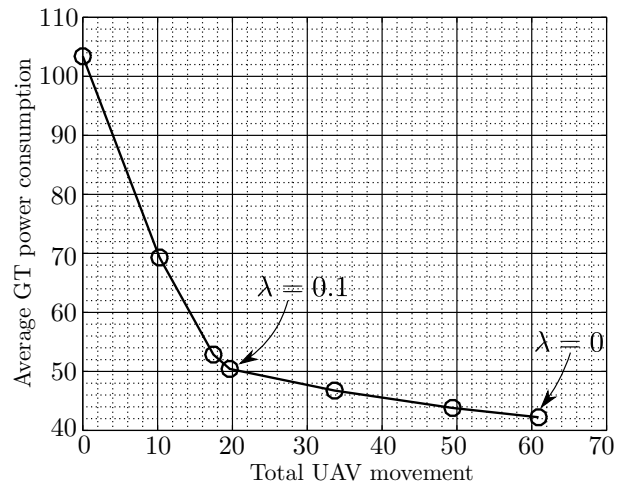


Fig. 7. Total movement vs. power consumption for a two-dimensional network.

ACKNOWLEDGEMENTS

The authors would like to thank Raheleh Khodabakhsh and Nitin Surya for their invaluable feedback on an earlier version [17] of this paper.

VI. CONCLUSIONS AND EXTENSIONS

We have studied the optimal deployment and relocation of UAV networks. We have first considered the case of variable ground terminal (GT) transmission power with fixed data rate. We have found the asymptotically optimal UAV locations that minimize the average GT power consumption. We have also provided analytical and numerical methods for dynamic UAV deployment. In particular, we have found the asymptotically optimal UAV trajectories for one-dimensional networks.

Let us finally discuss the case of variable-rate fixed-power systems. In this case, each GT transmits with a fixed power P , resulting in the achievable average rate (in nats/sec/Hz)

$$R(\mathbf{x}, f) \triangleq \int_{\mathbb{R}^d} \log \left(1 + \frac{P}{(\min_i \|x_i - q\|^2 + h^2)^{\frac{r}{2}}} \right) f(q) dq, \quad (37)$$

as the variable-rate analogue of (1). For a large number of UAVs, a Taylor series expansion yields

$$R(\mathbf{x}, f) = \log \left(1 + \frac{P}{h^r} \right) - \frac{\frac{1}{2}rP/h^2}{P+h^r} \int_{\mathbb{R}^d} \min_i \|x_i - q\|^2 f(q) dq + \int_{\mathbb{R}^d} o(\min_i \|x_i - q\|^2) f(q) dq. \quad (38)$$

This final expression is in the same form as (12); the only differences are in the constants. All of our results thus extend to variable-rate systems in a straightforward manner.

REFERENCES

- [1] Y. Zeng, R. Zhang, and T. J. Lim, "Wireless communications with unmanned aerial vehicles: Opportunities and challenges," *IEEE Commun. Mag.*, vol. 54, no. 5, pp. 36–42, May 2016.
- [2] I. Bor-Yaliniz and H. Yanikomeroglu, "The new frontier in RAN heterogeneity: Multi-tier drone-cells," *IEEE Commun. Mag.*, vol. 54, no. 11, pp. 48–55, Nov. 2016.
- [3] R. I. Bor-Yaliniz, A. El-Keyi, and H. Yanikomeroglu, "Efficient 3-D placement of an aerial base station in next generation cellular networks," *IEEE Intl. Conf. Commun.*, May 2016.
- [4] E. Kalantari, H. Yanikomeroglu, and A. Yongacoglu, "On the number and 3D placement of drone base stations in wireless cellular networks," *IEEE Veh. Tech. Conf.*, Sept. 2016.
- [5] J. Lyu, Y. Zeng, R. Zhang, and T. J. Lim, "Placement optimization of UAV-mounted mobile base stations," *IEEE Commun. Lett.*, vol. 21, no. 3, pp. 604–607, Mar. 2017.
- [6] J.-S. Marier, C.-A. Rabbath, and N. Léchevin, "Health-aware coverage control with application to a team of small UAVs," *IEEE Trans. Control Sys. Tech.*, vol. 21, no. 5, pp. 1719–1730, Sept. 2013.
- [7] Y. Zeng and R. Zhang, "Energy-efficient UAV communication with trajectory optimization," *IEEE Trans. Wireless Commun.*, vol. 16, no. 6, pp. 3747–3760, June 2017.
- [8] Y. Zeng, R. Zhang, and T. J. Lim, "Throughput maximization for UAV-enabled mobile relaying systems," *IEEE Trans. Commun.*, vol. 64, no. 12, pp. 4983–4996, Dec. 2016.
- [9] K. Anazawa, P. Li, T. Miyazaki, and S. Guo, "Trajectory and data planning for mobile relay to enable efficient Internet access after disasters," *IEEE Global Commun. Conf.*, Dec. 2015.
- [10] P. Zhan, K. Yu, and A. L. Swindlehurst, "Wireless relay communications with unmanned aerial vehicles: Performance and optimization," *IEEE Trans. Aerospace Elect. Sys.*, vol. 47, no. 3, pp. 2068–2085, July 2011.
- [11] F. Jiang and A. L. Swindlehurst, "Optimization of UAV heading for the ground-to-air uplink," *IEEE J. Select. Areas Commun.*, vol. 30, no. 5, pp. 993–1005, June 2012.
- [12] R. M. Gray and D. L. Neuhoff, "Quantization," *IEEE Trans. Inf. Theory*, vol. 44, no. 6, pp. 2325–2383, Oct. 1998.
- [13] A. Okabe, B. Boots, K. Sugihara, and S. N. Chiu, *Spatial Tessellations: Concepts and Applications of Voronoi Diagrams*, 2nd ed., Wiley Series in Probability and Statistics. New York, NY: John Wiley & Sons, 2000.
- [14] E. Koyuncu, "Performance gains of optimal antenna deployment for massive MIMO systems," *IEEE Global Commun. Conf.*, Dec. 2017.
- [15] Y. Song, B. Wang, Z. Shi, K. R. Pattipati, and S. Gupta, "Distributed algorithms for energy-efficient even self-deployment in mobile sensor networks," *IEEE Trans. Mobile Comput.*, vol. 13, no. 5, pp. 1035–1047, May 2014.
- [16] E. Koyuncu and H. Jafarkhani, "On the minimum average distortion of quantizers with index-dependent distortion measures," *IEEE Trans. Signal Process.*, vol. 65, no. 17, pp. 4655–4669, Sept. 2017.
- [17] E. Koyuncu, R. Khodabakhsh, N. Surya, and H. Seferoglu, "Deployment and trajectory optimization for UAVs: A quantization theory approach," *IEEE Wireless Commun. Networking Conf.*, Apr. 2018.
- [18] P. L. Zador, "Asymptotic quantization error of continuous signals and the quantization dimension," *IEEE Trans. Inf. Theory*, vol. 28, no. 2, pp. 139–148, Mar. 1982.
- [19] P. A. Chou, T. Lookabaough, and R. M. Gray, "Entropy-constrained vector quantization," *IEEE Trans. Acoustics, Speech and Signal Process.*, vol. 37, no. 1, pp. 31–42, Jan. 1989.
- [20] S. P. Lloyd, "Least squares quantization in PCM," *IEEE Trans. Inf. Theory*, vol. 28, no. 2, pp. 129–137, Mar. 1982.
- [21] Y. Linde, A. Buzo, and R. Gray, "An algorithm for vector quantizer design," *IEEE Trans. Commun.*, vol. 28, no. 1, pp. 84–95, Jan. 1980.
- [22] p.s. (<https://math.stackexchange.com/users/17433/p-s>), "min : sum of L2 norm and squared-L2 norm," *Mathematics Stack Exchange*, [Online] Available: <https://math.stackexchange.com/q/931702> (version: 2014-09-15).